J. Opt. B: Quantum Semiclass. Opt. **2** (2000) 299–305. Printed in the UK PII: S1464-4266(00)09831-1

Non-classical properties of even circular states

R Ragi†‖, B Baseia‡ and S S Mizrahi§

† Instituto de Física, Universidade de São Paulo, PO Box 66318, São Paulo, 05315-970, SP, Brazil
‡ Instituto de Física, Universidade Federal de Goiás, PO Box 131, Goiânia, 74001-970, GO, Brazil
§ Departamento de Física, CCET, Universidade Federal de São Carlos, PO Box 676, São Carlos, 13565-905, SP, Brazil

E-mail: rragi@quantum.sel.eesc.sc.usp.br

Received 23 November 1999, in final form 7 April 2000

Abstract. Here we investigate some general properties of the so-called *even circular state* (ECS) produced in a cavity, consisting of a superposition of N coherent states $|\alpha_k\rangle$ ($k = 1, 2, \ldots, N$) with the same $|\alpha_k|$. Several special states may emerge from this kind of superposition: in particular, when $1 \ll (e|\alpha_k|^2/N)^N \ll 4^N$ a Fock state with N quanta is produced, whereas when $(e|\alpha_k|^2/N)^N \ll 1$ one gets a vacuum state. We analyse the atomic scattering the ECSs produce when two-level atoms go through the cavity and also the *non-classical depth* of these states.

Keywords: Circular states, atomic scattering, non-classical depth

1. Introduction

The non-classical properties of quantum states of the radiation field have been thoroughly investigated by several authors as reported in the literature. They are now standard topics in many textbooks [1–3]. Two essential questions occur when one considers these kinds of states, namely, '*how non-classical is a quantum state?*' and in order to classify these states '*could they be ordered according to the value of some parameter that would reflect the degree of their non-classical character?*'. In this direction, we cite the pioneering works by Hillery [4], Lee [5] and Lutkenhaus and Barnett [6], discussing the concept of the *non-classical depth* of a quantum state. In this paper we focus our attention on a special class of states as introduced in [7–10]. This class concerns a sum of N coherent states $\sum_{k=1}^{N} F_k|\alpha_k\rangle$, all having the same amplitude $|\alpha_k| = r$; however, they are distributed with equal probability on a circle in phase space. For that reason they are called *circular states*. Here we shall consider, in particular, the case $F_k = 1$, the *even circular state* (ECS). For $N > 1$ this state is no longer coherent and is non-classical, since, according to Hillery [4], any pure state which is not coherent is a quantum state. So, it is interesting to determine the degree of the non-classical character of the ECSs as a function of N and the other parameters involved. Our results and discussions are presented in four additional sections. In section 2 we present the ECS of the electromagnetic (EM) field; we analyse the statistical properties of this field, as the photon number distribution, the average number of photons and variance, in terms of a defined partition function; asymptotic ($N \gg 1$) results are presented; we also calculate and depict the Wigner function since it permits us to get a deeper insight of the properties of this field. In section 3 we discuss the connection between the atomic scattering produced by the field in this state and by the field in the number state or by the vacuum state. In section 4 we study the non-classical depth parameter of the field that classifies the ECSs for different values of N. Section 5 contains a summary of our results and additional comments.

2. Even circular states

As is well known, a single coherent state is a pure quantum state which lies on a borderline, where on one side one has the states of the EM field that present properties defined as classical, and on the other, the so-called quantum states having properties defined as non-classical (antibunching, sub-Poissonian statistics, squeezed states, etc). The EM field represented by a state written as a superposition of two coherent states no longer belongs to the borderline because it shows non-classical properties. Many contributions on discrete superposition of coherent states have already been reported [7–10]. One main result concerns the properties coming from the interference, in phase space, between the various components involved in the superposition. When the radiation field is intense, the superposition is called the *Schrödinger cat* state [11], which can exhibit several non-classical effects. The production of such states by distinct nonlinear optical processes were investigated in [12]; in a recent paper by Szabo *et al* [8] it was shown that an

‖ Present address: Escola de Engenharia de São Carlos, Departamento de Engenharia Elétrica, USP, PO Box 359, 13560-970, São Carlos, SP, Brazil.

arbitrary quantum state of the field can be approximated by a superposition of coherent states located on a circle in phase space.

The more popular Schrödinger 'cat' states are the even (+) and odd (−) superpositions of coherent states, $N = 2$ [13],

$$|\Psi_{\pm}\rangle = \eta_{\pm}[|\alpha\rangle \pm |-\alpha\rangle], \tag{1}$$

where $\eta_{\pm}$ is the normalization factor and $\{|\alpha\rangle, |-\alpha\rangle\}$ are coherent states. One generalization of state (1) is the ECS defined as [7]

$$|\Psi_N\rangle = \eta'_N \sum_{k=1}^{N} |\alpha_k\rangle, \qquad N = 2, 3, 4, \ldots \tag{2}$$

where N is an integer standing for the number of coherent states

$$|\alpha_k\rangle = \mathrm{e}^{-r^2/2} \sum_{n=0}^{\infty} \frac{\alpha_k^n}{\sqrt{n!}} |n\rangle$$

present in the superposition, with

$$\alpha_k = r\mathrm{e}^{\mathrm{i}\theta_k}, \qquad \theta_k = \theta_0 + 2\pi k/N,$$

and η'_N is the normalization factor. It is easy to verify that in terms of the number states basis the ECS (2) can be written as

$$|\Psi_N\rangle = \eta_N \sum_{k=0}^{\infty} \frac{\alpha_0^{Nk}}{\sqrt{(Nk)!}} |Nk\rangle, \tag{3}$$

where $\alpha_0 = r\mathrm{e}^{\mathrm{i}\theta_0}$. Thus the ECS (3) is a superposition of number states that are elements of the countable subset $\{|0\rangle, |N\rangle, |2N\rangle, \ldots\}$. Calling $\eta_N = [Z(N, y)]^{-1/2}$ where $y \equiv r^2$, one identifies

$$Z(N, y) = \sum_{k=0}^{\infty} \frac{y^{Nk}}{(Nk)!} \tag{4}$$

as the *partition function*, which is the fundamental quantity containing the complete information on the statistical properties of the field.

2.1. Statistical properties of the ECS: photon number probability, mean and variance

The photon number probability for the ECS can be calculated by the usual form

$$P_n(N, y) = |\langle n|\Psi_N\rangle|^2 = \delta_{n,Nk} \frac{1}{Z(N, y)} \frac{y^n}{n!},$$
$$k = 0, 1, 2, \ldots \qquad N = 2, 3, 4, \ldots. \tag{5}$$

So, for a given number N, the photon number that can be found in the cavity will be a multiple of N. For instance, for $N = 4$, only $n = 0, 4, 8, \ldots$ photons can be found in the cavity with finite probability $P_0(4, y)$, $P_4(4, y)$, $P_8(4, y), \ldots$; for photon number $n \neq Nk$, $P_{n\neq Nk}(N, y) = 0$ due to destructive interference. We can now study the 'topography' of these states.

For $k = 1$, the 3D plot of $P_N(N, y)$ in figure 1(a) shows a very interesting result: the probability $P_N(N, y)$ is maximum for $N = y$; however, for a certain range of values of N and y, $P_N(N, y)$ is nearly equal to 1, which corresponds to the observed plateau. Thus, any pair of values (N, y) on the plateau means that the ECS is very close to a number state, $|\Psi_N\rangle \approx |N\rangle$. Hence, the present scheme suggests an alternative way for realizing a number state. At the right side of the plateau one notes the presence of a sharp cliff and then a plain for which $P_N(N, y) \approx 0$. This is a region where the ECS is very nearly a vacuum state, $|\Psi_N\rangle \approx |0\rangle$, due to the destructive interference in phase space, as will be discussed below. Then the two adjacent regions, the plateau and plain separated by a sharp cliff, show a transition between a high number state $|N\rangle$ and the vacuum state $|0\rangle$ as the values of N and y being changed.

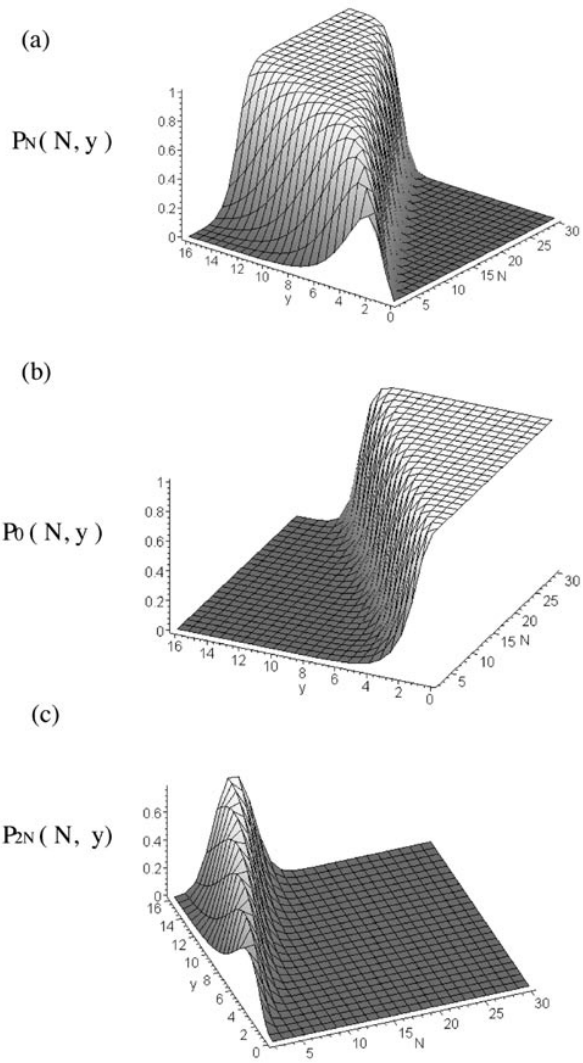

Figure 1. The photon number distribution $P_{n=N}(N, y)$ for $k = 1$; (b) $P_{n=0}(N, y)$ for $k = 0$; (c) $P_{n=2N}(N, y)$ for $k = 2$.

For $k = 0$, figure 1(b) shows the 3D plot of $P_0(N, y)$. Here we also verify the occurrence of a plateau ($P_0(N, y) \approx 1$) for high values of N and comparatively small values of y, corresponding to the probability of a vacuum state, and a plain ($P_0(N, y) \approx 0$) for all other values of the pair (N, y), this plain being the probability of a no-vacuum state. However, for $k > 1$ the plateaux no longer occur—see figure 1(c), where we present the same plot as figures 1(a) and (b) but for $k = 2$.

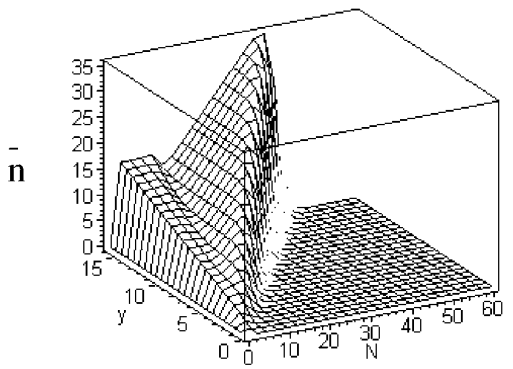

Figure 2. Average photon number $\bar{n}(N, y)$.

Next, we obtain for the average photon number

$$\bar{n}(N, y) \equiv \langle \Psi_N | \hat{n} | \Psi_N \rangle = \sum_{k=0}^{\infty} (Nk) P_{Nk} = y \frac{\partial}{\partial y} \log Z(N, y). \tag{6}$$

In general, the mean value for any power of $\hat{n}$ can be calculated from the following relation:

$$\overline{n^k} = \frac{1}{Z(N, y)} \left(y \frac{\partial}{\partial y} \right)^k Z(N, y).$$

Other quantities of interest for determining the field statistics are the variance $\mathrm{Var}(\hat{n}) \equiv \overline{n^2} - (\bar{n})^2$ and the Mandel Q parameter [1], defined as $Q \equiv (\mathrm{Var}(\hat{n}) - \bar{n})/\bar{n}$, which after some minor algebra can be written as

$$\mathrm{Var}(\hat{n}) = y \frac{\partial \bar{n}}{\partial y}, \qquad Q = y \frac{\partial \log \bar{n}}{\partial y} - 1. \tag{7}$$

Figure 2 shows the 3D plot of the mean number $\bar{n}(N, y)$, the flat slope at 45° meaning that $\bar{n}(N, y)$ increases proportionally to N. It corresponds to the flat plateau of figure 1(a), representing the realization of the number state $|N\rangle$, whereas the plain at the right of the cliff corresponds to the realization of the vacuum state since $\bar{n}(N, y) \approx 0$. The abrupt cliff shows the sharp transition from a number state with a high number of photons N to a vacuum state. The average excitation of the superposition state $|\Psi_N\rangle$ reaches a maximum for a certain value of N, and when the number of coherent states in the superposition increases beyond this value, the average number $\bar{n}(N, y)$ decreases rapidly. For a fixed value of y the minimum value $N = N_0$ for which the average number $\bar{n}(N, y)$ is near zero can be obtained by a simple calculation. Considering the first two terms in equation (4) we obtain $N_0 \simeq 1 + ey$. For the case $y = 4$, $N_0 \simeq 12$ we have $P_0 \simeq 0.9$. When $N > N_0$ the average number $\bar{n}(N, y)$ for these states is near zero and $P_0(N, y) \simeq 1$.

2.2. Field statistics

The parameter Q was introduced by Mandel and Wolf [1] for classifying the statistics of the EM fields: for $Q < 0$ the field has a sub-Poissonian statistics, for $Q = 0$ a Poissonian statistics and for $Q > 0$ the statistics is super-Poissonian. In figure 3 we can see several plots of $Q(N, y)$ versus N, for different values of y; this quantity oscillates between sub- and super-Poissonian statistics when N increases and these oscillations increase when y increases. However, when $N \gg 1$ and $y/N < 1$ the parameter Q starts to increase linearly with N although the variance $\mathrm{Var}(\hat{n})$ becomes null! This can be understood through the analysis of the asymptotic expressions for $N \gg 1$ and $y/N < 1$. In this case the partition function has the following approximate expression:

$$Z(N, y) \approx 1 + \frac{y^N}{N!}, \tag{8}$$

and the other quantities become (setting $k = 1$)

$$P_N(N, y) \approx \frac{y^N}{N!(1 + y^N/N!)} \tag{9}$$

$$\bar{n}(N, y) \approx \frac{N(y^N/N!)}{1 + y^N/N!} \tag{10}$$

$$\mathrm{Var}(\hat{n}) \approx \bar{n}(N - \bar{n}); \qquad Q \approx N - \bar{n} - 1. \tag{11}$$

Thus, as $\bar{n} \to 0$, we note that $\mathrm{Var}(\hat{n}) \to 0$ but $Q \to N - 1$, showing different limit values. On the left side of figure 4 one sees the 3D plot of $\mathrm{Var}(\hat{n})$ where the right and left plains (with respect to the main peak) correspond to regions of vacuum and number states, respectively. On the right side of the same figure we have a top view, where the shaded regions correspond to $\mathrm{Var}(\hat{n}) = 0$, so corroborating the above discussion on figure 1. In figure 5 we present the plot of $\mathrm{Var}(\hat{n}) - \bar{n}$ where one sees that when the mean photon number $\bar{n} \to 0$ (vacuum state) one gets $\mathrm{Var}(\hat{n}) \to 0$, suggesting a Poissonian statistics. However, adopting the strict definition for the classification of each kind of statistics using Mandel's parameter Q, one gets the limit $Q \to N$, showing that this vacuum can be said to have a super-Poissonian statistics.

The Wigner function for the ECSs was calculated and depicted together with the contour levels for pairs of values (N, y) picked at the centre of the plateau in figure 1(a): figure 6(a) stands for (12, 10) for which the probabilities $P_{n=Nk}(N, y)$, photon mean value $\bar{n}(N, k)$ and variance $\mathrm{Var}(\hat{n})$ are presented in table 1. One verifies that the $k = 1$ term is dominant in the sum of equation (3). In figure 6(b) we depicted the Wigner function and its contour levels for the number states, $|12\rangle$, and we see a striking discrepancy between states $|\tilde{N}\rangle$ and $|N\rangle$. From these results we see that there is a special class of ECSs that may be called *approximate number states*, denoted by $|\tilde{N}\rangle$; in particular, the first two states in table 1 are $|\tilde{12}\rangle$ and $|\tilde{20}\rangle$. Thus, in spite of the *approximate number states* and the number states presenting likely statistics, because of the interference effects in phase space their Wigner functions differ significantly, showing that the Wigner function is quite sensitive to 'tiny' deviations between the two states. The ECS for the pair (20, 16), presents statistics even closer to a number state (see table 1) but its Wigner function is quite similar to that of figure 6(a).

In the region of vacuum states ($k = 0$ term in equation (3) or the plain in figure 1(a)) the Wigner function shows a close similarity to that obtained for the vacuum state $|0\rangle$: in figure 7(a) we plotted the Wigner function and its contour levels for the state $|\tilde{0}\rangle$, corresponding to the pair (15, 3), that we compare with the Wigner function for $|0\rangle$, depicted in

Table 1. The first column stands for the pairs of values of N and y; the second to fourth columns show the probabilities for $n = 0, N, 2N$ photons; the fifth and sixth columns show the mean number and photon variance.

(N, y)	$P_0(k=0)$	$P_N(k=1)$	$P_{2N}(k=2)$	$\bar{n}$	$\mathrm{Var}(\hat{n})$
(12, 10)	0.000 478	0.998 700	0.000 771	12.003 500	0.179 900
(20, 16)	0.000 002	0.999 994	0.000 004	20.000 032	0.002 247
(15, 3)	0.999 989	0.000 011	0	0.000 165	0.002 469
(20, 3)	1.000 000	0	0	0	0
(25, 5)	1.000 000	0	0	0	0

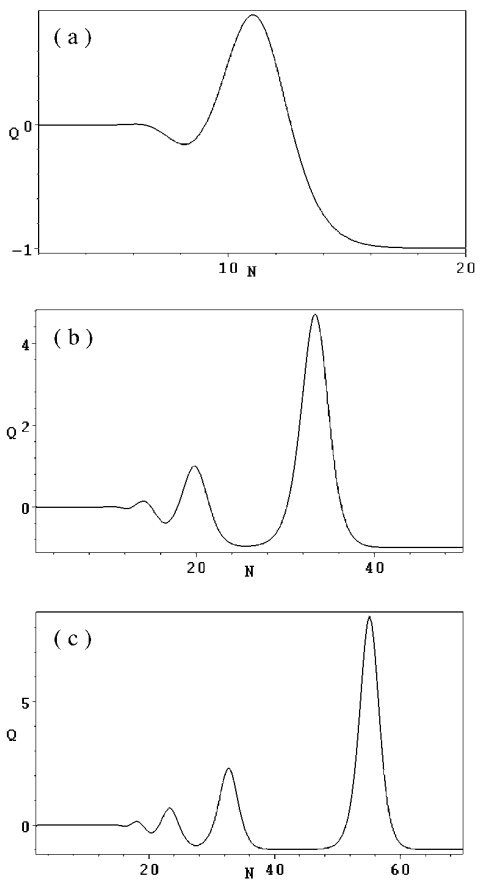

Figure 3. Mandel parameter $Q(N, y)$ as a function of N for various values of r: (*a*) $y = 16$; (*b*) $y = 49$ and (*c*) $y = 81$.

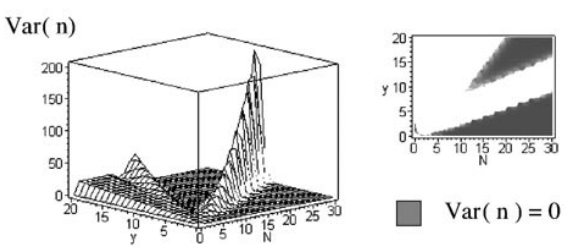

Figure 4. Variance $\mathrm{Var}(\hat{n})$ as a function of N and y; on the right side is a top view of this figure.

figure 7(*b*). The other two ECSs (20, 3) and (25, 5) also reproduce very closely the Wigner function figure 7(*b*): they can also be denoted as $|\tilde{0}\rangle$.

In summary, besides showing the usual properties of the superposition of typical coherent states, for a fixed value

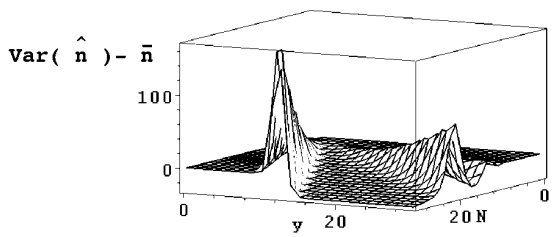

Figure 5. $\mathrm{Var}(\hat{n}) - \bar{n}$ as a function of N and y.

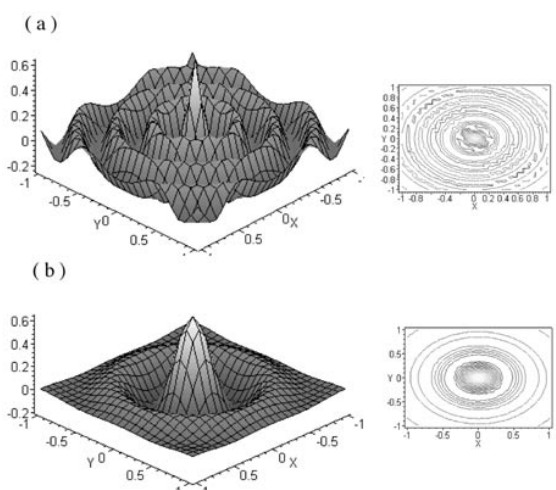

Figure 6. On the left side is the 3D plot of the Wigner function and on the right one sees its contour levels for (*a*) the ECS $N = 20$, $y = 16$; (*b*) the number state $|20\rangle$.

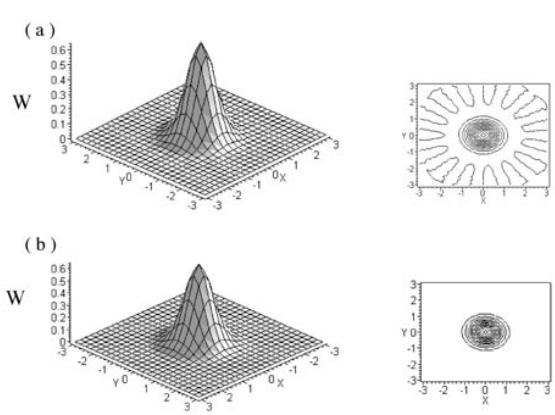

Figure 7. The same as in figure 6: (*a*) the ECS $N = 15$, $y = 3$; (*b*) the vacuum state $|0\rangle$.

of r there is a set of values $S_{\tilde{N}} = \{N, y\}$ for which the terms of the ECS interfere in a special fashion, thus giving

an approximate number state $|\Psi(S_{\tilde{N}})\rangle \equiv |\tilde{N}\rangle \approx |N\rangle$ for $1 \ll (ey/N)^N \ll 4^N$. Yet, for another set of values $S_{\tilde{0}} = \{N, y\}$, the state $|\Psi(S_{\tilde{0}})\rangle \equiv |\tilde{0}\rangle \approx |0\rangle$ is an almost vacuum state that occurs for $(ey/N)^N \ll 1$. It is worth paying attention to the following state construction: setting $N = 10$ and $y = 3.68$, for instance, one gets the truncated expansion

$$|\Psi_{N=10}\rangle \approx \frac{1}{\sqrt{2}}[|0\rangle + |10\rangle], \tag{12}$$

with all other terms in the expansion very close to zero. Thus, particular values of y and N allow the approximate truncation of the infinite series to the first two terms. Also, one can choose y and N conveniently to get a superposition of states $|kN\rangle$ and $|(k+1)N\rangle$; so it is possible to get a superposition of two Fock number states by interference in phase space of the superposition of N coherent states. As a related matter, we draw attention to a recent proposal to generate a *truncated state*, an equal weight superposition of states $|0\rangle$ and $|1\rangle$ [14]: the method was named 'quantum scissors' and it concerns travelling waves.

3. Atomic scattering

Let us suppose that it is possible to create experimentally an ECS in a cavity as proposed in [8]. Then one asks 'How could these states affect the scattering spectrum of two-level Rydberg atoms going through the cavity near the node of the stationary field?'. This section is therefore devoted to obtaining such a spectrum. Assuming that a high-Q cavity sustains the first harmonic, the atom-field interaction is given by $V = -\mu\mathcal{E}_0 \sin(kx)(\hat{\sigma}^+\hat{a} + \hat{\sigma}^-\hat{a}^+)$, k is the wavenumber of the mode and x is the coordinate perpendicular to the direction of the atomic beam. Here we follow the scheme introduced by Freyberger and Herkommer [15]. The expression for the probability density $W(\wp)$ of finding the scattered atom with transverse momentum $\wp = p/\hbar k$, is given by [15]

$$\begin{aligned} W(\wp) &= \langle\Phi(\wp, t)|\Phi(\wp, t)\rangle = 2|\tilde{f}(\wp)|^2|C_0|^2 \\ &+ \sum_{m=1}^{\infty}[|\tilde{f}(\wp - \kappa\sqrt{m})|^2|C_m + \mathrm{e}^{\mathrm{i}\varphi}C_{m-1}|^2 \\ &+ |\tilde{f}(\wp + \kappa\sqrt{m})|^2|C_m - \mathrm{e}^{\mathrm{i}\varphi}C_{m-1}|^2] \end{aligned} \tag{13}$$

where $\kappa = \mu\mathcal{E}_0\tau/\hbar$ is the interaction parameter, τ is the interaction time,

$$C_m = \delta_{m,Nk}\eta_N\frac{\alpha_0^m}{\sqrt{m!}}, \qquad N = 2, 3, \ldots, \quad k = 0, 1, 2, \ldots$$

are the coefficients of the ECS expanded in the number state basis, $\tilde{f}(\cdot)$ is the Fourier transform of

$$f(x) = \frac{1}{(\pi\sigma^2)^{\frac{1}{4}}}\mathrm{e}^{-\frac{x^2}{2\sigma^2}}$$

which is the spatial distribution of atoms in a narrow beam entering the cavity, i.e. where $\sigma = \Delta x$ is the width of the Gaussian lineshape of this atomic beam, and

$$\tilde{f}(\wp \pm \kappa\sqrt{m}) = \left(\frac{\sigma^2}{16\pi\hbar^2}\right)^{\frac{1}{4}}\mathrm{e}^{-\frac{k^2\sigma^2}{2}(\wp\pm\kappa\sqrt{m})^2}.$$

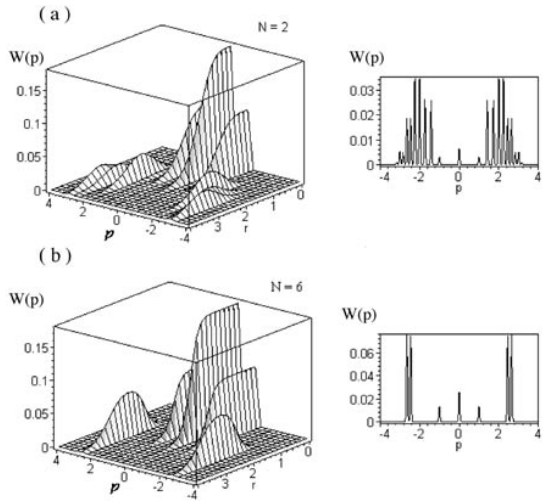

Figure 8. On the left side we have plotted the probability density $W(\wp, N, r)$ as a function of the transverse momentum $\wp = p/(\hbar k)$ and r, for $\kappa = 30$, $\varphi = 0$; on the right side we have plotted cut planes for $r = 2$. (*a*) $N = 2$; (*b*) $N = 6$.

The 3D plots of the atomic scattering distribution function $W(\wp, N, r)$ are shown on the left side of figure 8. We considered $\kappa = 30$, $\varphi = 0$ and $N = 2, 6$; transverse cuts in these figures for $r = 2$ are shown on the right side. These figures exhibit two symmetrical groups of peaks, and the probability $W(\wp, N, r)$ increases with N for a fixed value of r. When $N \gg r$ the probability distribution $W(\wp, N, r)$ coincides with the atomic scattering produced by a vacuum state, as it should, because $|\tilde{0}\rangle \approx |0\rangle((ey/N)^N \ll 1)$. Now it is quite interesting to analyse what happens with the atomic scattering for a field in the cavity being an almost number state ($1 \ll (ey/N)^N \ll 4^N$) and to compare the scattering pattern with the one produced by the number state $|N\rangle$. Thus, although the Wigner functions for $|N\rangle$ and $|\tilde{N}\rangle$ present discrepancies, the spectrum of the atomic scattering cannot distinguish between the two states of the field. The scattering produced by a number state $|N\rangle$,

$$\begin{aligned} W(\wp) &= 2|\tilde{f}(\wp)|^2\delta_{N,0} + |\tilde{f}(\wp - \kappa\sqrt{N})|^2 \\ &+ |\tilde{f}(\wp + \kappa\sqrt{N})|^2 + \left|\tilde{f}\left(\wp - \kappa\sqrt{N+1}\right)\right|^2 \\ &+ \left|\tilde{f}\left(\wp + \kappa\sqrt{N+1}\right)\right|^2 \end{aligned}$$

displays a characteristic profile, always having two pairs of peaks placed not exactly symmetrically, whose position depends on the number of photons N, as we can see in figure 9. The same is verified for the approximate vacuum state $|\tilde{0}\rangle$, where the probability $W(\wp, 0, r)$ is indistinguishable from that obtained from the vacuum state $|0\rangle$.

4. Non-classical depth of the state $|\Psi_N\rangle$

The motivation to study the non-classical character of a state comes from the necessity of knowing how non-classical a state of the radiation field is. However, it is not trivial to obtain this non-classical character since the quantum nature of a radiation field arises in many

different ways [16]. Thus, for a long time the work on quantum optics was concerned with verifying whether or not a certain field state is non-classical, without any immediate interest in defining a degree of *non-classicality* or *non-classical depth*. Lee [5] introduced a method based on the convolution transformation between the quasiprobability distribution functions P (Glauber–Sudarshan function) and Q (Husimi function), which permitted one to measure the *non-classicality* of the field state in terms of a continuous parameter τ defined in the interval [0, 1]. Lee introduced the distribution function

$$R(z,\tau) = \frac{1}{1-\tau}\exp\left(\frac{1}{1-\tau}|z|^2\right)\frac{1}{\pi}\int \mathrm{d}^2u\langle -u|\hat{\rho}|u\rangle \times \exp\left[-\frac{1}{1-\tau}[(2\tau-1)|u|^2+(z^*u-zu^*)]\right], \quad (14)$$

where, for some value of τ, $R(z,\tau)$ exists as an ordinary function and is positive definite. The knowledge of $R(z,\tau)$ allows one to classify the non-classical states. When $\tau \simeq 0$, $R(z,\tau)$ stands for a nearly classical state, whereas when $\tau \simeq 1$ the state is strongly non-classical. Thus, we are in possession of a powerful tool for investigating the *non-classicality* of any pure state of the radiation field. To find the non-classical depth of the ECS $|\Psi_N\rangle$ we use equation (14) to get

$$R(z,\tau) = \sum_{j=1}^{N}\tilde{R}_{j,j}(z,\tau) + 2\sum_{k=1}^{N}\sum_{j(>k)=1}^{N}\tilde{R}_{j,k}(z,\tau),$$

where

$$\tilde{R}_{j,k}(z,\tau) = \frac{1}{1-\tau}\exp\left(\frac{1}{1-\tau}|z|^2\right)\frac{1}{\pi}\int \mathrm{d}^2u\langle -u|\rho_{j,k}|u\rangle \times \exp\left[-\frac{1}{1-\tau}[(2\tau-1)|u|^2+(z^*u-zu^*)]\right], \quad (15)$$

with

$$\langle -u|\rho_{j,k}|u\rangle = \eta_N^2\exp\left(-|u|^2-\frac{(|\alpha_j|^2+|\alpha_k|^2)}{2}+(u\alpha_k^*-u^*\alpha_j)\right). \quad (16)$$

The substitution of equation (15) in equation (16) gives, after some algebra,

$$\begin{aligned}\tilde{R}_{j,k}(z,\tau) &= \frac{\eta_N^2}{\tau}\exp\left\{-r^2-\frac{|z|^2}{\tau}-\left[\frac{1-\tau}{\tau}r^2\cos(\theta_j-\theta_k)\right]\right\}\\ &\quad\times\exp\{r|z|[\cos(\gamma-\theta_k)+\cos(\gamma-\theta_j)]\}\\ &\quad\times\left\{\cos\left[\frac{1-\tau}{\tau}r^2\sin(\theta_j-\theta_k)\right]\right.\\ &\quad\times\cos\left[\frac{|z|r}{\tau}\sin(\gamma-\theta_k)\right]\cos\left[\frac{|z|r}{\tau}\sin(\gamma-\theta_j)\right]\\ &\quad+\cos\left[\frac{1-\tau}{\tau}r^2\sin(\theta_j-\theta_k)\right]\\ &\quad\times\sin\left[\frac{|z|r}{\tau}\sin(\gamma-\theta_k)\right]\sin\left[\frac{|z|r}{\tau}\sin(\gamma-\theta_j)\right]\\ &\quad-\sin\left[\frac{1-\tau}{\tau}r^2\sin(\theta_j-\theta_k)\right]\\ &\quad\times\cos\left[\frac{|z|r}{\tau}\sin(\gamma-\theta_k)\right]\sin\left[\frac{|z|r}{\tau}\sin(\gamma-\theta_j)\right]\\ &\quad+\sin\left[\frac{1-\tau}{\tau}r^2\sin(\theta_j-\theta_k)\right]\\ &\quad\left.\times\sin\left[\frac{|z|r}{\tau}\sin(\gamma-\theta_k)\right]\cos\left[\frac{|z|r}{\tau}\sin(\gamma-\theta_j)\right]\right\}. \quad (17)\end{aligned}$$

Analysing a computer animation of the function $R(z,\tau)$ as a function of $|z|$ and τ for $\gamma \in [0, 2\pi]$, we were able to find the minimum value of τ yielding a positive definite function $R(z,\tau)$, for any value of $z = |z|\mathrm{e}^{\mathrm{i}\gamma}$. In this way, choosing several values of N we found the value of τ, thus obtaining its dependence on N. Figure 10 shows the plot of the *non-classical depth* parameter τ versus N for $r = 2$. We see that for $N < N_0$, $\tau \simeq 1$. For $N > N_0$, τ decreases, and $\tau \to 0$, when $N \gg N_0$. This is an interesting result since it shows that the vacuum state emerges from the ECSs. Hence, the number of coherent states constituting our superposition state $|\Psi_N\rangle$ establishes a constraint upon its *non-classicality*. This constraint also depends on the parameter r. When $r > 2$, the height of the initial plateau in figure 10 diminishes and the curve dips for larger values of N.

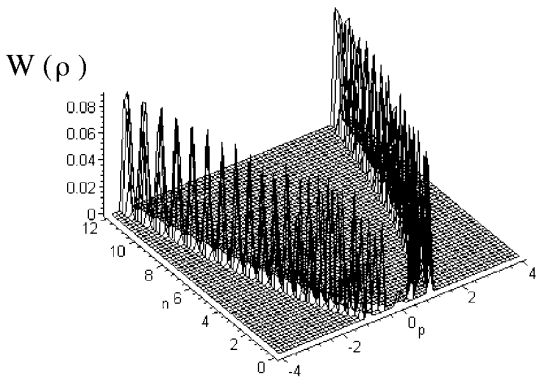

Figure 9. The probability density $W(\wp)$ obtained for the number state $|N\rangle$.

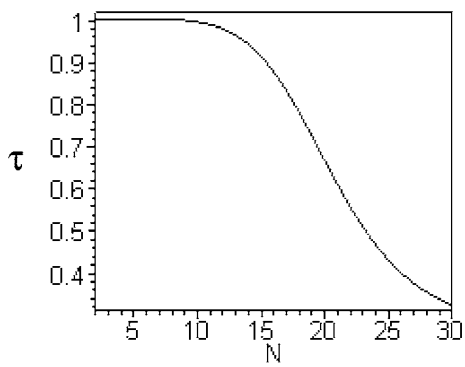

Figure 10. The non-classical depth parameter τ as a function of N for $r = 2$.

5. Summary and comments

We have studied a particular class of quantum states of a field in a cavity, the ECSs, which showed very unusual properties that depend on the number N of coherent states that are superposed and on the parameter r; for large values of N they

allow one to realize an almost number state $|\tilde{N}\rangle$ or an almost vacuum state $|\tilde{0}\rangle$, besides other superpositions of number states. However, we have focused our attention mainly on these states. The ECS exhibits various non-classical effects: the number of photons allowed in the cavity is a multiple of N $\{0, N, 2N, 3N, \ldots\}$ with exactly zero probability of finding any other number of photons that do not belong to this set. For values of r and N such that $1 \ll (ey/N)^N \ll 4^N$, the ECSs become approximately a number state, since in this region $P_N(N, y) \approx 1$. The mean photon number $\overline{n}(N, y)$ as well as the variance $\mathrm{Var}(\hat{n})$ agree with this analysis. Concerning the atomic scattering by a field in state $|\Psi_N\rangle$ in a cavity which reproduces approximately states $|N\rangle$ or $|0\rangle$, we noted that the probability distribution for the transverse momentum cannot be distinguished from the one produced by the exact states. However, the corresponding Wigner functions for $N \neq 0$ do not coincide, due to the quantum interference in phase space, with all statistical properties coinciding. Thus, presumably we have shown a simple scheme to generate a number state (or a vacuum state) from a superposition of N coherent states, for adequate values of N and y.

Concerning the non-classical depth τ of our state $|\Psi_N\rangle$, we have shown that τ goes from $\tau \simeq 1$ (highly non-classical) to $\tau \simeq 0$ (almost classical) when N goes from $N < N_0$ to $N \gg N_0$. When N is in the region where our $|\Psi_N\rangle$ is almost a number state $|\tilde{N}\rangle$ the value of τ is maximum and when it approaches a vacuum state $|\tilde{0}\rangle$, $\tau = 0$.

As a final remark we mention that the generation of an ECS can be obtained via the application of the 'standard' quantum state engineering, by passing $(N-1)$ Rydberg atoms through a high-Q cavity to generate the superposition of N coherent states, as defined in equation (2). In the present case, we must prepare each atomic state entering the cavity, the latter initially prepared in a coherent state $|\alpha_1\rangle$, and we should also make a convenient choice of the traversing time of atoms through the cavity (corresponding to a choice of the atomic velocity). A preliminary (straightforward, but tedious) calculation using a dispersive interaction allows us to anticipate that: the jth atom should enter the cavity previously prepared (in a first Ramsey zone) in the state $|\Psi(0)\rangle_A = \eta(\xi_{j,N}|e\rangle_j + |g\rangle_j)$, where η is a normalization factor, $\xi_{j,N} = -\mathrm{e}^{-2ij\pi/N}$, $j = 1, 2, 3, \ldots, (N-1)$, and the traversing time corresponding to a phase $\phi_N = 2\pi/N$ has originated from dispersive interaction. A detailed calculation, including a comparison with other recurrence formulae for the resonant interaction, is found in [17].

As a related matter we note that three schemes for generating circular states and Fock number states for the vibrational motion of a trapped ion are presented in [18].

Acknowledgments

RR thanks useful discussions with Professor Vanderlei S Bagnato, from the IFSC-USP. This paper was partially supported by FAPESP (São Paulo, SP) and CNPq (Brasília, DF), Brazilian agencies.

References

[1] Mandel L and Wolf E 1995 *Optical Coherence and Quantum Optics* (Cambridge: Cambridge University Press)
[2] Scully and Zubairy 1997 *Quantum Optics* (Cambridge: Cambridge University Press)
[3] Walls D F and Milburn G J 1994 *Quantum Optics* (Berlin: Springer)
[4] Hillery M 1985 *Phys. Lett.* A **111** 409
[5] Lee C T 1991 *Phys. Rev.* A **44** R2775
Lima A F and Baseia B 1996 *Phys. Rev.* A **54** 4589
[6] Lutkenhaus N K and Barnett S M 1995 *Phys. Rev.* A **51** 3340
[7] Gagen M J 1995 *Phys. Rev.* A **51** 2715
[8] Szabo S, Adam P, Janszky J and Domokos P 1996 *Phys. Rev.* A **53** 2698
[9] Janszky J, Domokos P and Adam P 1993 *Phys. Rev.* A **48** 2213
[10] Domokos P, Janszky J, Adam P and Larsen T 1994 *Quantum Opt.* **6** 187
[11] Janszky J and Vinogradov An V 1990 *Phys. Rev. Lett.* **64** 2771
Buzek V and Knight P L 1991 *Opt. Commun.* **81** 331
Buzek V, Vidiella-Barranco A and Knight P L 1992 *Phys. Rev.* A **45** 6570
[12] Yurke B and Stoler D 1986 *Phys. Rev. Lett.* **57** 13
Milburn G J 1986 *Phys. Rev.* A **33** 674
Milburn G J and Holmes C A 1986 *Phys. Rev. Lett.* **56** 2237
Kitagawa M and Yamamoto Y 1986 *Phys. Rev.* A **34** 3974
Mecozzi A and Tombesi P 1987 *Phys. Rev. Lett.* **58** 1055
Wolinsky M and Carmichael H J 1988 *Phys. Rev. Lett.* **60** 1836
Kennedy T A B and Drummond P D 1988 *Phys. Rev.* A **38** 1319
Savage C M and Cheng W A 1989 *Opt. Commun.* **70** 439
Savage C M, Braunstein S L and Walls D F 1990 *Opt. Lett.* **15** 628
[13] Gerry C C and Hach E E III 1993 *Phys. Lett.* A **174** 185
Gerry C C and Hach E E III 1993 *Phys. Lett.* A **179** 1
Dodonov V V, Malkin I A and Man'ko V I 1994 *Physica* **72** 597
Dodonov V V, Man'ko V I and Nikonov D E 1995 *Phys. Rev.* A **51** 3328
Zaheer K and Wahiddin M R B 1994 *J. Mod. Opt.* **41** 151
[14] Pegg D T, Phillips L S and Barnett S M 1998 *Phys. Rev. Lett.* **81** 1604
[15] Freyberger M and Herkommer A M 1994 *Phys. Rev. Lett.* **72** 1952
Baseia B, Vyas R, Dantas C and Bagnato V S 1994 *Phys. Lett.* A **194** 153
Baseia B, Marques G C and Bagnato V S 1995 *Phys. Lett.* A **200** 7
Vaglica A 1995 *Phys. Rev.* A **52** 2397
[16] Loudon R 1980 *Rep. Prog. Phys.* **43** 58
Teich M C and Saleh B E A 1988 *Progress in Optics* vol 26, ed E Wolf (Amsterdam: North-Holland) pp 1–104
Zou X T and Mandel L 1990 *Phys. Rev.* A **41** 475
[17] Moussa M H Y and Baseia B 1998 *Phys. Lett.* A **238** 223
[18] José W D and Mizrahi S S 2000 *J. Opt. B: Quantum Semiclass. Opt.* **2** 306